



## Full Length Article

Nonlinear behavior during NO<sub>2</sub> hydrogenation on a nanosized Pt-Rh catalyst sampleCédric Barroo <sup>a,b,\*</sup>, Yannick De Decker <sup>b,c,1</sup>, Luc Jacobs <sup>a</sup>, Thierry Visart de Bocarmé <sup>a,b,\*</sup><sup>a</sup> Chemical Physics of Materials and Catalysis, Université libre de Bruxelles (ULB), Faculty of Sciences, CP243, 1050 Brussels, Belgium<sup>b</sup> Interdisciplinary Center for Nonlinear Phenomena and Complex Systems (CENOLI), Université libre de Bruxelles (ULB), Faculty of Sciences, 1050 Brussels, Belgium<sup>c</sup> Non Linear Physical Chemistry Unit, Université libre de Bruxelles (ULB), Faculty of Sciences, CP231, 1050 Brussels, Belgium

## ARTICLE INFO

## Article history:

Received 9 January 2017

Received in revised form 29 March 2017

Accepted 30 March 2017

Available online 31 March 2017

## Keywords:

Pt-Rh

Nonlinear behavior

Catalyst

NO<sub>2</sub>

Field emission microscopy

## ABSTRACT

Automotive pollution control crucially relies on the reactivity of metal alloy catalysts. Understanding how the chemistry of an alloy compares with that of pure metals forms a decisive step towards the rational development of applied formulations of such catalysts. In this context, we studied the hydrogenation of NO<sub>2</sub> on Pt-Rh catalysts at the nanoscale with field emission microscopy (FEM). Previous studies have shown the presence of complex reaction kinetics at the surface of Pt for this reaction, including periodic oscillations at 390 K. As we briefly show here, similar kinetics can also be observed on Rh at higher temperatures. The alloy samples (Pt-17.4 at.%Rh) show signs of important reactivity and associated nonlinear dynamics in an intermediate temperature range. In particular, at 425 K isothermal oscillations are observed on this specific alloy catalyst. The role of the alloy composition on the window of reactivity is explained with a simple theoretical model for the kinetics of the reaction.

© 2017 Elsevier B.V. All rights reserved.

## 1. Introduction

In the past decades, surface science techniques have been widely used to reach a better understanding of the mechanisms of reactions of interest in the automotive pollution control by catalysis. CO oxidation on platinum samples is by far the most studied system on extended facets of single crystals [1–3], as well as on samples presenting facets with several different crystallographic orientations [4–6]. Another important class of reactions is the selective catalytic reduction of nitrogen oxides (NO<sub>x</sub>) over platinum group metals. DeNOx reactions such as NO + CO [7] or NO + H<sub>2</sub> [8–10] have been studied extensively on pure metals. However, despite its crucial importance in air pollution control, NO<sub>2</sub> reduction has not been studied in great detail [11,12]. Recent work from our group provided in this context an in-depth analysis of the complex kinetics occurring during NO<sub>2</sub> hydrogenation at the surface of Pt field emitter tips. Aperiodic oscillations, monomodal and bimodal periodic oscillations, as well as propagation of front waves have for example been observed [13–16]. Similar results have also been obtained for

the NO<sub>2</sub> + H<sub>2</sub> reaction on Rh field emitter tips and will be presented in this paper.

Most of these studies were performed on pure metallic samples. However, the applied formulations of catalysts are mostly made of alloys such as Pt-Rh binary alloys. The fundamental study of such reactive systems is challenging because the catalyst may undergo morphological reconstructions and because the chemical composition of its very first atomic layers can change, so that the surface composition is expected to considerably differ from that of the bulk. Surface segregation can for example be triggered by a change of temperature, by a modification of the nature of the gas phase, or by successive physicochemical treatments of the surface of the catalyst [17–19]. The simultaneous determination of the morphology of the catalyst, its surface composition as well as its activity and selectivity is therefore experimentally difficult and hardly predictable by current theoretical methods.

The only deNOx reaction studied so far on extended facets of Pt-Rh binary alloys is the NO + H<sub>2</sub> reaction, which has been addressed by Nieuwenhuys and coworkers [10]. Their work suggests a lack of synergy between Pt and Rh: the differences in terms of catalytic activity with respect to the pure metals are explained by the surface composition and the activity of each metal for the given reaction [20]. Comparative studies have been conducted and indicate that the use of Rh-10 at.%Pt significantly decreases the dissociation rate of NO as compared to pure Rh, which would result from the lower capability of Pt to dissociate NO [21,22].

\* Corresponding authors at: Chemical Physics of Materials and Catalysis, Université libre de Bruxelles (ULB), Faculty of Sciences, CP243, 1050 Brussels, Belgium.

E-mail addresses: [cbarroo@ulb.ac.be](mailto:cbarroo@ulb.ac.be) (C. Barroo), [tvisart@ulb.ac.be](mailto:tvisart@ulb.ac.be)

(T.V. de Bocarmé).

<sup>1</sup> These authors contributed equally.

From a dynamical point of view, alloy catalysts exhibit behaviors that are similar to those of pure metal catalysts: thermokinetic oscillations have been studied on Pt-Rh [23–25], and a bistable regime has been reported for CO oxidation on a Pd-Cu(110) catalyst [26]. Also, bimetallic samples such as micro-composite catalysts made of Pt and Rh allow for the observation of propagating fronts of reaction [27]. Purely isothermal oscillations have been observed in a limited number of reactive systems on alloys [28,29]. This type of oscillations can be studied at the nanoscale in a field emission microscope where the temperature of the sample is controlled and kept constant during the whole process.

## 2. Results and discussion

In this paper, we describe experiments using field electron emission microscopy (FEM) (Methods) to image the ongoing processes occurring at the surface of single nanoparticles of catalyst via brightness analysis of specific regions of interest (ROIs) of the FEM pattern. These ROIs correspond to facets with well-defined crystallographic orientations. The probed area corresponds to approximately  $10\text{--}20\text{ nm}^2$ . As the  $\text{NO}_2 + \text{H}_2$  reaction has already been studied on Pt field emitter tips [13–16], we focus in this work on the case of Rh and on Pt-17.4 at.%Rh samples. Isothermal self-sustained periodic oscillations have been observed for the pure metals and also in the case of a binary alloy. The next sections are devoted to a phenomenological description of self-sustained periodic oscillations on Rh samples, the characterization of Pt-Rh sample, as well as the observation of “surface explosions” and nonlinear reaction behavior on Pt-Rh. This system is then compared to results obtained on pure Pt and pure Rh samples, and observations are explained by using a qualitative reaction mechanism that contains the essential features of the system.

### 2.1. Nonlinear reaction behavior on Rh

We first describe the dynamics of the catalytic hydrogenation of  $\text{NO}_2$  on pure Rh samples and compare these results with our previous investigations on pure Pt. Our experiments focus on the study of  $\text{NO}_2 + \text{H}_2$  reaction by Field Electron Microscopy (FEM) on samples conditioned as sharp tips. By its size and morphology, the apex is a relevant model bearing the structural features of a single catalytic particle. FEM is based on the emission of electrons from the sample when the tip-sample is negatively charged as compared to the detector screen. The emission of electrons depends on the local work function at the surface, which depends on the crystallographic orientation of the facets and the presence of different adsorbates, but also on the local electric field. FEM micrographs thus represent a mapping of the convolution of the local work function and local electric field over the surface. For a given temperature and applied field, the current density of field emitted electrons is ruled by the distribution of local fields and the work function, which can vary upon the presence of adsorbates. FEM can thus be used to qualitatively follow the presence of adsorbates at the surface. It has to be noted that while local changes of the surface composition result in variations of the local brightness, no conclusion can be drawn regarding the activity of facets where there is no measurable variation of brightness, i.e. when facets are and remain dark.

The procedure consists in the characterization of the sample with atomic lateral resolution by field ion microscopy (FIM) at low temperature ( $\sim 50\text{ K}$ ), followed by FEM analysis at working temperature. A base pressure of  $\text{NO}_2$  is then introduced in the reaction chamber. The presence of oxygen atoms is known to increase the work function on rhodium [30,31]. The dissociative adsorption of  $\text{NO}_2$  thus leads to a decrease in image brightness, but only at locations on the surface where decomposition of this species

occurs. The  $\text{H}_2$  pressure is then increased in a stepwise fashion until occurrence of a “surface explosion” is observed. The term “surface explosion” (or “explosion”) here refers to the catalytic light-off, or catalytic ignition, of the reaction, which corresponds to a kinetic transition from a state of low activity to a state of high activity. In our case, adsorbate-species react together and the subsequent products of reaction desorb concurrently on all the visible facets within a time resolution of the recording device of 50 fps (frames per second). The formation of products and their fast desorption induce a rapid increase of the local brightness. This fast catalytic ignition is thus referred to as “surface explosion” in the remaining of this manuscript. The facets presenting variations in the brightness signal during the reaction appear to be the  $\{011\}$  facets and their close neighbors, namely  $\{012\}$  facets, as well as some  $\{113\}$  facets. Changes in brightness can be related to changes of surface composition, as discussed earlier, which implies that these facets are chemically active. Conversely, the  $\{001\}$  and  $\{111\}$  facets remain dark for the whole duration of the reaction, which could either mean that there is no chemical activity, or that the imaging process in FEM does not allow to observe reactivity on these specific facets because the variations of brightness are weaker than what the recording device can detect.

This observation corresponds to a fast clean-off of the adsorbates layer which is made visible by a fast increase of the brightness signal of the screen of the microscope. This increase can be associated with the presence of either  $\text{H}_2\text{O}$  or  $\text{NH}_3$  species. Indeed, these two species induce a decrease of the work function [32–34]. By analogy with experiments on Pt catalysts [13], the reaction on Rh may be expected to lead primarily to the production of water. However, Rh is also known for its ability to dissociate  $\text{NO}(\text{ads})$  species. The more probable dissociation of  $\text{NO}(\text{ads})$  on Rh with respect to Pt may induce the presence of  $\text{N}(\text{ads})$  species, which can undergo a successive addition of mobile hydrogen atoms to form  $\text{NH}_3$  in the presence of an excess of dihydrogen in the system.

The occurrence of successive “explosions” at the surface of the catalyst at constant control parameters corresponds to an unstable regime, which takes here the form of self-sustained periodic oscillations. A characteristic time series obtained during such self-sustained periodic oscillations on a  $\{011\}$  Rh facet at  $450\text{ K}$  is represented in Fig. 1a. We can observe rather large variations in the amplitude of the peaks, which vary between 40 and 120 levels of brightness within a grey scale of 256 steps. The fluctuations of the peak amplitudes are most likely due to the small size of the studied system. Fig. 1b corresponds to a magnification over five oscillations highlighting the asymmetric shape of the peak. This asymmetry is preserved throughout the whole time series, whatever the amplitude of the peak.

A single oscillation can be divided into three parts:

- A transition period of low brightness that lasts approximately  $25\text{ s}$  which can be associated to the presence of  $\text{O}(\text{ads})$  species;
- A sharp increase in brightness within a short time interval due to the removal of the adsorbed layer, which releases products;
- A slower decrease in brightness lasting  $\sim 10\text{ s}$  after which the brightness drops back to its initial value. This decrease can be attributed to the dissociative adsorption of  $\text{NO}_2(\text{g})$ , releasing oxygen atoms.

The oscillations can thus be seen as relaxation-type oscillations in the sense that the “stress” accumulated during the transition period is relaxed during a short “discharge”. The “stress” we refer to can be considered to be related to the chemical force (in the thermodynamic sense) due to the accumulation of adsorbed reactants at the surface, while the “relaxation” part would correspond to the catalytic light-off, involving both fast reactions and desorption. The periodicity of the process is determined by power spectrum analy-

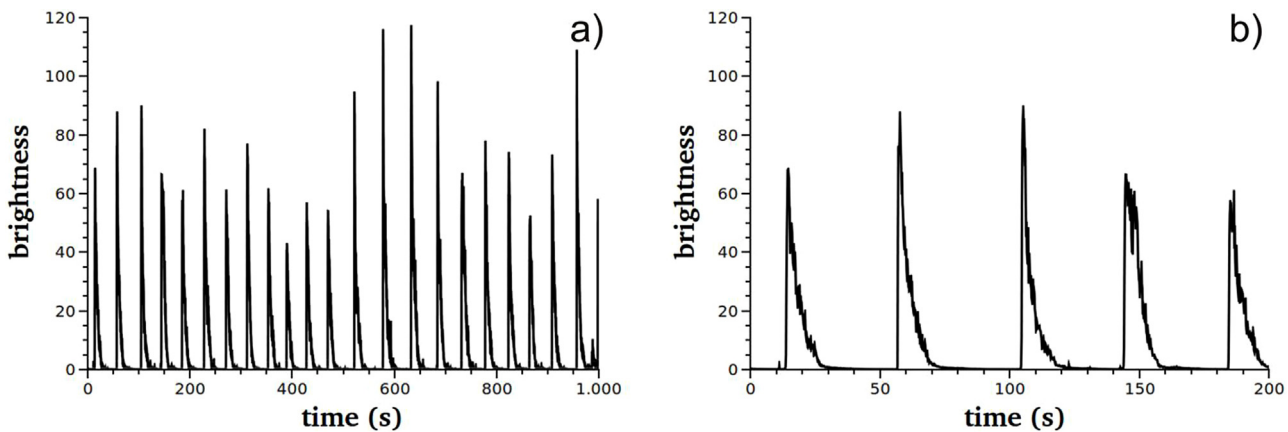


**Fig. 1.** (a) Brightness signal representing self-sustained periodic oscillations on a {011} Rh facet during  $\text{NO}_2 + \text{H}_2$  reaction with a period of 42.1 s (conditions:  $T = 450\text{ K}$ ,  $F \approx 4\text{ V nm}^{-1}$ ,  $P_{\text{NO}_2} = 2.93 \times 10^{-5}\text{ Pa}$ ,  $P_{\text{H}_2} = 7.28 \times 10^{-4}\text{ Pa}$ ). (b) Enlargement on five peaks of oscillations allowing for the observation of the detailed shape of the peak (relaxation-type oscillations) as well as of the importance of fluctuations. Brightness is expressed in units spanning over the grayscale defined by the 8 bits coding each pixel.

ses and shows a period of 42.1 s (0.0237 Hz). The period can range however from some 40–50 s as a function of the hydrogen pressure. Note that most of the oscillations observed on Pt present a much shorter periodicity ranging between 2 and 14 s [15]. The normalized autocorrelation function (the case of Pt is presented Fig. S1) presents oscillations with a decaying envelope, which confirms that the system corresponds to a noisy oscillator. The correlation time of the oscillations,  $\tau_c$ , which is the time for the envelope to decrease to a value of 1/e, is of 48.94 s (1.16 periods of oscillation) for the example considered here. The ratio of this correlation time to the period of oscillations is a universal indicator of the robustness of an oscillating system. Although the robustness of the oscillator is less than in the case of Pt, these results are consistent with general theoretical predictions on the correlation time of nano-sized systems [35]. A complete analysis of the  $\text{NO}_2 + \text{H}_2$  reaction on Rh – including bifurcation analysis, reconstruction of dynamical attractor, as well as discussion of the mechanism – will be published separately.

Considering that self-sustained oscillations occur on pure Pt as well as on pure Rh samples, the question of the emergence of periodic behaviors on a Pt-Rh bimetallic alloy is raised, as well as the relationships of such phenomena to those observed on the pure metals.

## 2.2. Characterization of the Pt-17.4 at.%Rh sample

Pt-Rh samples were prepared by electrochemical etching (Methods) and a field ion micrograph of a {111}-oriented sample is presented on Fig. 2a. Pt and Rh both crystallize in the face-centered cubic crystal structure and their lattice parameters are 392 pm and 380 pm, respectively. The structure of the sample thus remains well defined at the atomic scale. Among other treatments, flash heating at 600 K under ultra-high vacuum conditions and field evaporation have been used. It has been previously proved that these conditions do not lead to any surface segregation [17] and the initial surface can therefore be considered as a homogeneous solid solution of Pt and Rh. As discussed in the introduction, this may no longer be true under reactive conditions. On Fig. 2b, a field emission micrograph is reproduced and we can observe that {012}-type facets are subject to field emission.

## 2.3. "Surface explosions" and nonlinear reaction behavior on Pt-Rh

Experiments on Pt-Rh samples have been conducted in the temperature range 390–515 K. The work function of Pt-17.4 at.%Rh sample has been determined to be  $\approx 5.0\text{ eV}$  [36]. Although no data

are available in the literature regarding changes in the work function after adsorption of  $\text{NO}_2$  on Pt-Rh surfaces, the introduction of nitrogen dioxide in the analysis chamber leads to a strong and fast decrease in brightness, as for pure Pt and Rh. This decrease is thus assigned to the dissociative adsorption of  $\text{NO}_2$  leading to  $\text{NO(ads)}$  and  $\text{O(ads)}$  species.

As mentioned, the procedure to observe isothermal "surface explosions" (i.e. the catalytic light-off) on Pt and Rh consists in the injection of a base pressure of  $\text{NO}_2$  in the analysis chamber followed by a gradual increase of the hydrogen pressure until a "surface explosion" occurs. During "surface explosions", only the {012} and {011} facets are bright whereas {113} facets remain dark. This observation is in line with the observation of brightness variations on both Pt and Rh. It is also in agreement with previous work on NO on Rh-25 at.%Pt, where it has been shown that the adsorption and dissociation of NO is sensitive to the surface structure and the activity for the NO hydrogenation follows the sequence: Pt-Rh (111) < (100) < (410) [37].

Single explosive phenomena have been observed in the whole investigated temperature range. The shape of the peaks of "explosions" displays a significant diversity depending on the temperature of the catalyst and the initial pressure of  $\text{NO}_2$ . However, for fixed conditions the general aspect of the peaks remains similar and the  $\text{H}_2$  pressure required to initiate the "explosions" stays in the same range. Contrary to the case of pure Pt and Rh sample, self-sustained oscillations, which translate into the occurrence of several successive "surface explosions" without any change in the control parameters, have been observed only in a limited range of pressures and temperatures. A typical time series of such oscillations can be found in Fig. 3a, while Fig. 3b focuses on five representative peaks. The minimum  $\text{NO}_2$  base pressure required to initiate periodic oscillations on the alloy is closer to what was observed on Pt ( $10^{-4}\text{ Pa}$ ) than on Rh ( $10^{-5}\text{ Pa}$ ). No oscillations could be observed for temperature below 425 K and above 475 K, which is to be contrasted with oscillations on pure Pt (390 K–515 K) and pure Rh (450 K–500 K).

As in the case of Rh, the fluctuations of amplitude are relatively important. The amplitude of the peaks ranges between 130 and 250 levels of brightness. The autocorrelation function is reproduced on Fig. 4b and the line corresponds to the 1/e value used to determine the correlation time  $\tau_c$ . The decrease of the envelope of the autocorrelation function is fast and  $\tau_c$  can be estimated to 6.6 s, half a period of oscillation. This robustness is low as compared to pure Pt for which  $\tau_c$  can be as long as hundreds of periods, but is similar to the range measured for pure Rh. The shape of the peaks is again characteristic of relaxation-type oscillations. We observe however

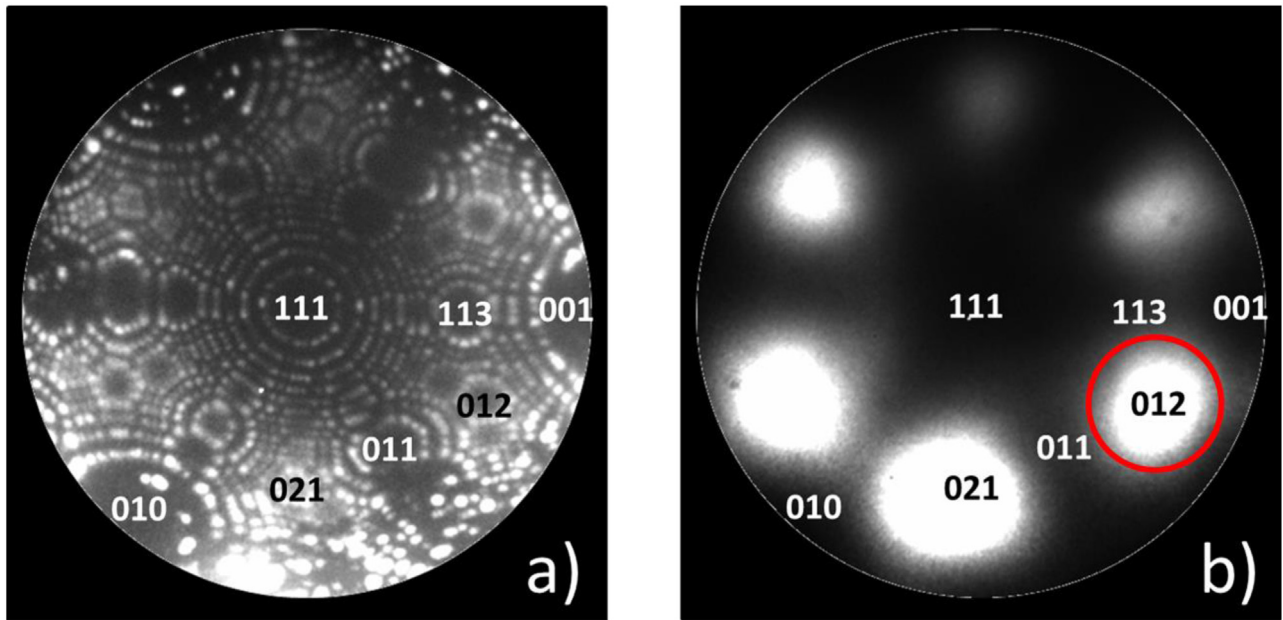


**Fig. 2.** Characterization of a Pt-17.4 at.%Rh sample. (a) Field ion microscopy pattern of a Pt-17.4 at.%Rh sample (111) oriented with its principal Miller indices (conditions: T = 60 K, P<sub>Ne</sub> = 2 × 10<sup>-3</sup> Pa, F ≈ 35 V nm<sup>-1</sup>). (b) Field emission microscopy pattern of the same sample under ultra-high vacuum conditions (conditions: T = 60 K, F ≈ 4 V nm<sup>-1</sup>). The red circle correspond to the (012) facet, ROI where the brightness signal was probed. (For interpretation of the references to color in this figure legend, the reader is referred to the web version of this article.)

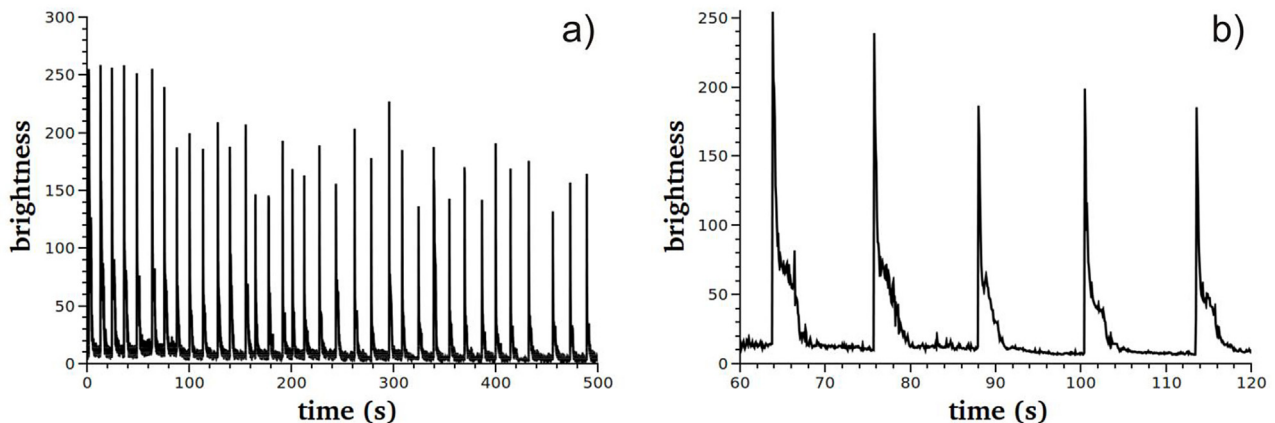


**Fig. 3.** (a) Brightness signal of self-sustained periodic oscillations on Pt-17.4 at.%Rh during NO<sub>2</sub> + H<sub>2</sub> reaction on a {012} facet (conditions: T = 425 K, F ≈ 4 V nm<sup>-1</sup>, P<sub>NO<sub>2</sub></sub> = 3.86 × 10<sup>-4</sup> Pa, P<sub>H<sub>2</sub></sub> = 1.43 × 10<sup>-2</sup> Pa). (b) Enlargement on five peaks of oscillations allowing the observation of the general shape of relaxation-type oscillations and the importance of fluctuations as in the Rh case. Brightness is expressed in units spanning over the grayscale defined by the 8 bits coding each pixel.

that the part of the oscillation cycle corresponding to a decrease in brightness differs from what can be seen on Rh (compare peaks on Figs. 1 b and 3 b). In the case of alloy samples, the brightness decreases abruptly and then reaches an almost constant transient lasting 7–9 s. The further decrease down to the initial brightness level – the one taking place just before the next surface “explosion” – occurs on a longer time scale. What happens during this two-stage transient is not known hitherto, but experiments by pulsed field desorption mass spectrometry [38] will help to reveal the surface composition during this plateau. Similar behaviors have been observed on pure Pt samples.

#### 2.4. Comparison with Pt and Rh

The general phenomenology of the NO<sub>2</sub> + H<sub>2</sub> reaction on Pt-17.4 at.%Rh is similar to the phenomenology on pure Pt and pure Rh:

- The dissociative adsorption of NO<sub>2</sub> induces a decrease in brightness of the field emission pattern due to an oxygen-induced increase in work function;
- “surface explosions” are observed, which can be associated to a fast reaction-induced emptying of the surface;
- In each case, the most visible regions during the ongoing reaction are {012} and {011} facets, while {111} facets remain dark;
- The single “surface explosions” and the occurrence of self-sustained oscillations have the form of relaxation-type kinetics.

However, a more detailed analysis reveals that the Pt-Rh system shows features that are borrowed either from Pt or from Rh:

- On one hand, the degree of robustness of the oscillations is close to what is observed on Rh;

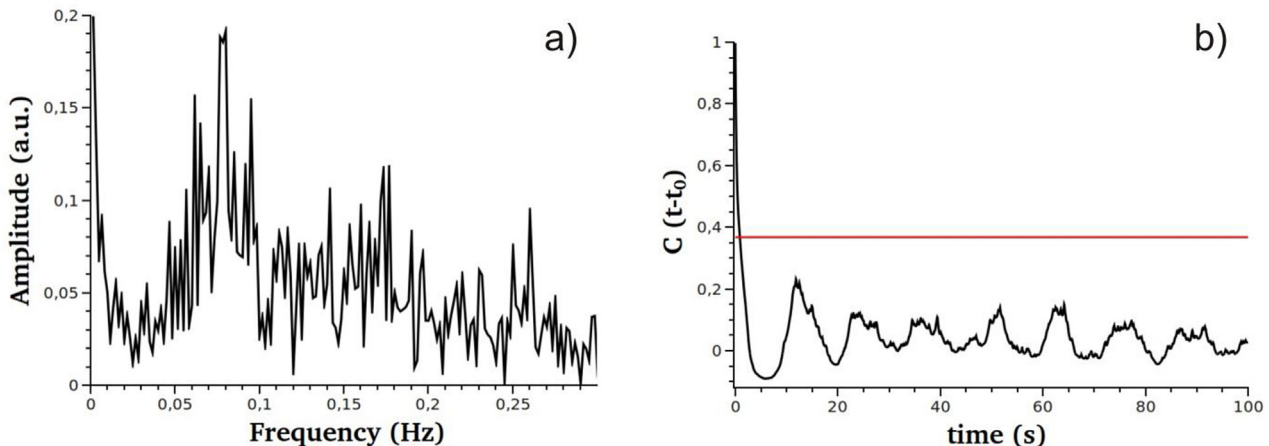
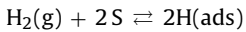
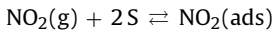


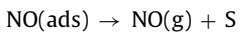
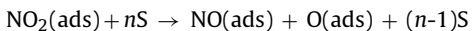
**Fig. 4.** (a) Power spectrum of the brightness signal presented Fig. 3 showing a frequency of 0.08 Hz. (b) Interval-dependent normalized correlation function showing oscillations with strong damping. The red line corresponds to  $1/e$  to determine the correlation time of 6.6 s (half a period). (For interpretation of the references to color in this figure legend, the reader is referred to the web version of this article.)

- On the other hand, the minimal pressure of  $\text{NO}_2$  necessary to initiate oscillations and the shape of the peaks are similar to those observed on Pt;
- Finally, the temperature range in which oscillations are observed lies at the intersection between those of pure Pt and pure Rh.

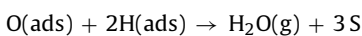
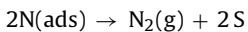
These similarities and differences raise the question of which factors control the reactivity of the alloy with respect to the pure metals. To assess this, we consider a qualitative reaction mechanism that contains the essential features of the system at hand. This model includes the molecular adsorption of  $\text{NO}_2$  and the dissociative adsorption of dihydrogen from the gas phase onto the surface:



Here, S stands for an empty active site (we consider all sites to be equivalent). Once on the surface,  $\text{NO}_2$  can decompose into NO and O and the NO released in this way can either desorb or dissociate as well,



Note that we consider the NO desorption to be irreversible, since its partial pressure is expected to be very small compared to those of the injected gases. It should also be noted that while it is usually considered irreversible, the decomposition of  $\text{NO}_2$  strongly depends on the amount of available empty sites ( $n > 1$ ) on the surface because it must bend towards empty surface regions to dissociate, as shown by DFT calculations on Pt [13]. A similar conclusion was shown to hold for NO as well ( $m > 1$ ) [39]. Moreover, the  $\text{NO}_2$  adsorption geometry and decomposition mechanism suggest that its dissociation becomes strongly hindered when the fraction of empty active sites goes below a critical value [13]. Finally, the model also includes reactions between adatoms to give  $\text{N}_2$  and water, respectively



Water is considered to desorb almost instantaneously, in accordance with the known life times of this molecule on the two metals at the temperatures of interest. Note that this model is a simplification of a previously introduced double-path mechanism developed to explain oscillations on Pt FEM samples at 390 K [13,14].

The corresponding evolution laws for the coverage of each species  $i$ ,  $[i]$ , read under the mean field assumption are:

$$\frac{d[\text{NO}_2]}{dt} = k_{\text{ads}}^{\text{NO}_2} [\text{S}]^2 - k_{\text{des}}^{\text{NO}_2} [\text{NO}_2]^2 - k_{\text{dec}}^{\text{NO}_2} [\text{NO}_2] F([\text{S}]) \quad (1)$$

$$\frac{d[\text{NO}]}{dt} = k_{\text{dec}}^{\text{NO}_2} [\text{NO}_2] F([\text{S}]) - 2k_{\text{des}}^{\text{NO}} [\text{NO}] - k_{\text{dec}}^{\text{NO}} [\text{NO}] [\text{S}]^m \quad (2)$$

$$\frac{d[\text{O}]}{dt} = k_{\text{dec}}^{\text{NO}_2} [\text{NO}_2] F([\text{S}]) + k_{\text{dec}}^{\text{NO}} [\text{NO}] [\text{S}]^m - k_r [\text{O}] [\text{S}]^2 \quad (3)$$

$$\frac{d[\text{N}]}{dt} = k_{\text{dec}}^{\text{NO}} [\text{NO}] [\text{S}]^m - 2k_{\text{des}}^{\text{N}_2} [\text{N}]^2 - 2k_w [\text{O}] [\text{H}]^2 \quad (4)$$

To obtain these equations, we used the fact that since all the processes involving adsorbed hydrogen are fast, an adiabatic elimination of this variable can be performed (see Supplementary information for more details). This has the consequence that the rate of formation of water is proportional to the square of the concentration of empty sites  $[\text{S}] = 1 - 2[\text{NO}_2] - [\text{NO}] - [\text{O}] - [\text{N}]$ , with an effective reaction rate constant  $k_r$  which is proportional to the  $\text{H}_2$  pressure. Moreover, to take into account the strong dependence of the  $\text{NO}_2$  dissociation on the empty sites, we use for  $F([\text{S}])$ :

$$F([\text{S}]) = [\text{S}]^n \quad \text{when } [\text{S}] \geq [\text{S}]_{\text{crit}} \\ = 0 \quad \text{otherwise}$$

Our basic assumption is that the evolution Eqs. (1) – (4) hold for pure metals as well as for alloys, the only difference being in the values taken by the different parameters. In accordance with experimental observations, this model predicts oscillations for a rather large range of parameter values (including the choice for  $m$ ,  $n$  and  $[\text{S}]_{\text{crit}}$ ). However, only a few parameters are expected to vary substantially as the atom fraction of rhodium changes. The two critical parameters in this view are the rate constants for NO dissociation ( $k_{\text{dec}}^{\text{NO}}$ ) and for  $\text{N}_2$  desorption ( $k_{\text{des}}^{\text{N}_2}$ ). Indeed, the value taken by these parameters strongly differ for Pt and Rh: for a given temperature, NO dissociation is more favorable on Rh, while  $\text{N}_2$  desorption is much more rapid on Pt. We will thus use  $k_{\text{dec}}^{\text{NO}}$  and  $k_{\text{des}}^{\text{N}_2}$  as control parameters, to determine how they can affect the

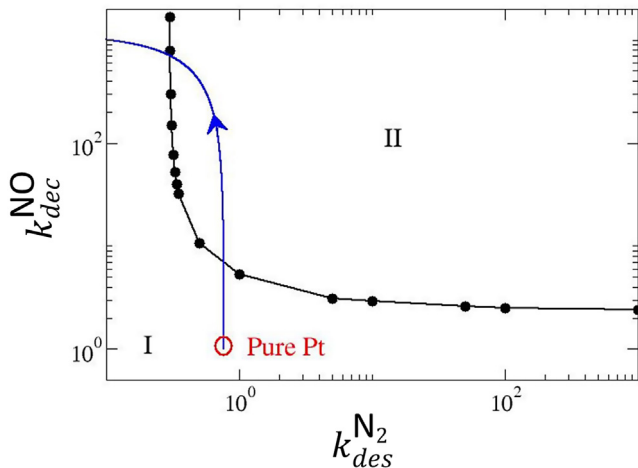


**Fig. 5.** Diagram showing the region of existence of sustained oscillations (region I) and the region where the system reaches a stationary state (region II). The black curve was computed for parameters corresponding to Pt(100) at 400 K (see Supplementary information for details), except for  $k_{ads}^{NO_2} = 0.6$  and for  $k_{des}^{NO_2} = 7.0$ . The blue curve corresponds to the values of  $k_{dec}^{NO}$  and  $k_{des}^{N_2}$  at the same temperature for an increasing Rh/Pt ratio within the alloy, as calculated from (5)–(6). (For interpretation of the references to color in this figure legend, the reader is referred to the web version of this article.)

properties of the oscillatory process. For simplicity, we assume that they both vary linearly with composition:

$$k_{dec}^{NO} = k_{dec}^{NO,Pt} \times (\text{at.\%Pt}) + k_{dec}^{NO,Rh} \times (\text{at.\%Rh}) \quad (5)$$

$$k_{des}^{N_2} = k_{des}^{N_2,Pt} \times (\text{at.\%Pt}) + k_{des}^{N_2,Rh} \times (\text{at.\%Rh}) \quad (6)$$

These assumptions are in line, for example, with observations that the addition of Pt to a Rh sample decreases the capacity to dissociate NO [21].

Fig. 5 shows the region (region I) where isothermal oscillations are observed as a function of  $k_{dec}^{NO}$  and  $k_{des}^{N_2}$  at  $T = 400$  K for a (100) facet (see Supplementary information for details on the calculation of the rate constants). Since there is no known experimental value for  $k_{ads}^{NO_2}$  and  $k_{des}^{NO_2}$ , these parameters were chosen so as to fit oscillations observed on Pt(100) at this temperature. The black curve on the graph corresponds to the values of  $k_{dec}^{NO}$  and  $k_{des}^{N_2}$  that separate oscillations from stationary coverages when all other parameters are maintained constant. To establish this curve, these two parameters were varied freely and they are thus not representative of a given metal or alloy. We also plotted in this figure the values taken by  $k_{dec}^{NO}$  and  $k_{des}^{N_2}$  as given by Eqs. (5) – (6) for (100) facets (blue curve). For pure Pt or Pt-rich alloys,  $k_{dec}^{NO}$  is fairly low while  $k_{des}^{N_2}$  is expected to be large and the dynamics of the system is oscillatory. As the fraction of Rh increases, the NO decomposition rate constant rapidly increases so that Rh-poor alloys are expected to present oscillations, while those that are too rich in Rh will simply lead to a constant concentration of adsorbates (since they correspond to region II). This is shown on Fig. 5 by following the blue curve starting from pure Pt at the bottom right. The difference in NO decomposition thus seems to be the main reason why oscillations are less likely to be observed on a Pt-Rh alloy as compared to pure Pt for a given temperature.

Time series corresponding to pure Pt, a Pt-20 at.%Rh alloy and pure Rh at 425 K are shown in Fig. 6. We observe that the model reproduces our observation that oscillations on the alloy have a shape that is similar to those observed on Pt, but with a different period, while no oscillation is seen for Rh. This can now be traced back to the fact that the alloy samples we used were poor in Rh, so that the parameter values are close to those of pure Pt. The period is

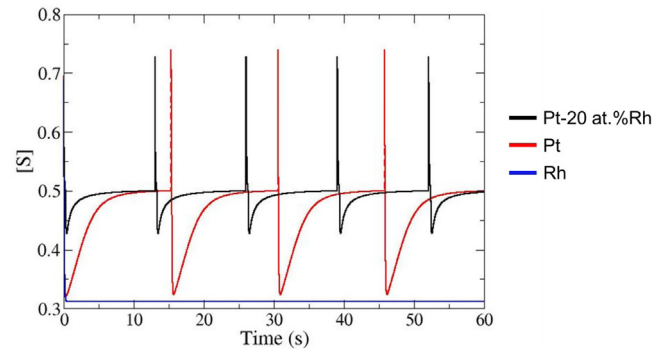


**Fig. 6.** Time series showing the temporal evolution of the fraction of empty sites [S]. The parameters correspond to Pt(100), now taken at 425 K (see Supplementary information), except for  $k_{ads}^{NO_2} = 1.0$  and for  $k_{des}^{NO_2} = 7.15$ , which were used as fitting parameters. The black curve corresponds to a Pt-20 at.%Rh alloy, the dotted red one to pure Pt and the blue one stands for pure Rh. (For interpretation of the references to color in this figure legend, the reader is referred to the web version of this article.)

nevertheless different on alloys because such samples correspond to a region of parameter space that is closer to the bifurcation line.

### 3. Conclusions

This study reveals the presence of pure isothermal self-sustained behaviors on Pt-Rh alloy, at the nanometer-scale level, and the characteristics of those oscillations lie between the features on pure Pt and pure Rh samples, which may be a sign of synergy between isolated metals. The existence of periodic oscillations during the  $\text{NO}_2 + \text{H}_2$  reaction on Pt, Rh as well as Pt-Rh samples suggest that the mechanism behind the occurrence of those oscillations is robust and seems to mostly depend on the reaction itself.

In the case of Rh experiments at 450 K, NO is more prone to dissociate on Rh so the products of reaction may be  $\text{H}_2\text{O}$  and/or  $\text{NH}_3$  species, as it has been highlighted on the  $\text{NO} + \text{H}_2$  system [10].

Regarding the reaction on Pt-Rh at 425 K, the products could be the same as in the Pt case, the same as in the Rh case, or a mix of both. Previous studies show that species such as  $\text{N}_2\text{O}$  and  $\text{NH}_3$  have been detected as products at temperatures ranging from 400 to 800 K on the Pt-Rh (100) facet in the case of  $\text{NO} + \text{H}_2$  reaction [40]. In our case, the decomposition of  $\text{NO}_2(\text{g})$  is supposed to hinder a successive decomposition of NO on Pt, Pd and Ru [41], and similarly, it is known that the presence adsorbed oxygen inhibits the adsorption and decomposition of  $\text{NO}_2(\text{g})$ . The reaction mechanism used is however in good agreement with the observation of oscillations on Pt, Rh and Pt-Rh and explains qualitatively the temperature range of these oscillations. Further studies are required to determine experimentally the exact nature of the products.

From a catalysis point of view, the use of tip-samples presenting a wide variety of facets with different crystallographic orientations – as compared to extended flat or stepped surfaces – allows bridging, to some extent, the materials-gap. A more detailed and systematic study of the surface composition and dynamical processes occurring, during the ongoing reaction, on pure metals and alloys of different composition could improve the understanding of synergistic effects between metals.

### 4. Methods

Principles and design of the field ion/electron microscope can be found in Ref. [42,43]. Rh and Pt-Rh field emitter tips were produced by electrochemical etching of metallic wires in a molten salt mixture of  $\text{NaCl}$  and  $\text{NaNO}_3$  (1/4 wt). The samples were subsequently cleaned inside the chamber of the microscope by cycles of

field evaporation, annealing and ion sputtering (see [14] for more details). In this way, a quasi-hemispherical tip was obtained, the size of which could be estimated by net plane counting between known orientations on the field ion micrograph. The reported dynamic behaviors were monitored by field electron microscopy in the presence of reactive mixtures of NO<sub>2</sub> and H<sub>2</sub> gases at 98 % (from Air Liquide) and 99.9999 % (from Praxair) purity respectively, at 450 K in the Rh case and 425 K in the Pt-Rh case. Times series were extracted from videos recorded with a Photron FastCam SA4 camera with a speed of acquisition of 50 fps (frame per second). Time series were established by probing the mean brightness over regions of interest by the software Photron Fastcam Viewer. Brightness is expressed in units spanning over the grayscale defined by the 8 bits coding each pixel.

## Author contributions

The manuscript was written through contributions of all authors. All authors have given approval to the final version of the manuscript.

## Acknowledgments

C.B. and L.J. thank the Fonds de la Recherche Scientifique (F.R.S.-FNRS) for financial support (Postdoctoral fellowship from FNRS and PhD grant from FRIA, respectively). The authors gratefully thank the Van-Buuren Foundation for a financial support for the acquisition of equipment and the Wallonia-Brussels Federation (Action de Recherches Concertées n°AUWB 2010–2015/ULB15).

## Appendix A. Supplementary data

Supplementary data associated with this article can be found, in the online version, at <http://dx.doi.org/10.1016/j.apsusc.2017.03.266>.

## References

- [1] G. Ertl, P.R. Norton, J. Rüstig, Kinetic oscillations in the platinum-catalyzed oxidation of CO, *Phys. Rev. Lett.* 49 (1982) 177–180.
- [2] G. Ertl, Reactions at surfaces: from atoms to complexity (Nobel lecture), *Angew. Chem. Int. Ed. Engl.* 47 (2008) 3524–3535.
- [3] M.M. Slin'ko, N.I. Jaeger, Oscillating heterogeneous catalytic systems, in: B. Delmon, J.T. Bates (Eds.), *Studies in Surface Science and Catalysis*, vol. 86, Elsevier, Amsterdam, 1994.
- [4] Yu. Suchorski, R. Imbihl, V.K. Medvedev, Compatibility of field emitter studies of oscillating surface reactions with single crystal measurements: catalytic CO oxidation on Pt, *Surf. Sci.* 401 (1998) 392–399.
- [5] Y. Suchorski, C. Spiel, D. Vogel, W. Draschel, R. Schlögl, G. Rupprechter, Local reaction kinetics by imaging: CO oxidation on polycrystalline platinum, *ChemPhysChem* 11 (2010) 3231–3235.
- [6] Yu. Suchorski, J. Beben, R. Imbihl, Local fluctuations during catalytic CO oxidation on Pt: a field emission study, *Surf. Sci.* 405 (1998) L477–L483.
- [7] Th. Fink, J.P. Dath, R. Imbihl, G. Ertl, The mechanism of kinetic oscillations in the NO + CO reaction on Pt(100), *Surf. Sci.* 251–252 (1991) 985–989.
- [8] M.F.H. van Tol, A. Gielbert, B.E. Nieuwenhuys, Oscillatory behavior of the reduction of NO by H<sub>2</sub> and NH<sub>3</sub> over Rh studied by FEM, *Appl. Surf. Sci.* 67 (1993) 179–187.
- [9] A.R. Cholach, M.F.H. van Tol, B.E. Nieuwenhuys, Origin of the spatiotemporal oscillations observed during the NO + H<sub>2</sub> reaction on a Rh field emitter, *Surf. Sci.* 320 (1994) 281–294.
- [10] N.M.H. Janssen, P.D. Cobden, B.E. Nieuwenhuys, Non-linear behaviour of nitric oxide reduction reactions over metal surfaces, *J. Phys.: Condens. Matter* 9 (1997) 1889–1917.
- [11] C. Voss, N. Kruse, Oscillatory behavior in the catalytic reduction of NO and NO<sub>2</sub> with hydrogen on Pt field emitter tips, *Appl. Surf. Sci.* 94/95 (1996) 186–193.
- [12] C. Voss, N. Kruse, Chemical wave propagation and rate oscillations during the NO<sub>2</sub>/H<sub>2</sub> reaction over Pt, *Ultramicroscopy* 73 (1998) 211–216.
- [13] J.-S. McEwen, P. Gaspard, Y. De Decker, C. Barroo, T. Visart de Bocarmé, N. Kruse, Catalytic reduction of NO<sub>2</sub> with hydrogen on Pt field emitter tips: kinetic instabilities on the nanoscale, *Langmuir* 26 (2010) 16381–16391.
- [14] C. Barroo, Y. De Decker, T. Visart de Bocarmé, N. Kruse, Complex oscillation patterns during the catalytic hydrogenation of NO<sub>2</sub> over platinum nanosized crystals, *J. Phys. Chem. C* 118 (2014) 6839–6846.
- [15] C. Barroo, Y. De Decker, T. Visart de Bocarmé, P. Gaspard, Fluctuating dynamics of nanoscale chemical oscillations: theory and experiments, *J. Phys. Chem. Lett.* 6 (2015) 2189–2193.
- [16] C. Barroo, Y. De Decker, T. Visart de Bocarmé, N. Kruse, Emergence of chemical oscillations from nanosized target patterns, *Phys. Rev. Lett.* 117 (2016) 144501.
- [17] P.A.J. Bagot, T. Visart de Bocarmé, A. Cerezo, G.D.W. Smith, 3D atom probe study of gas adsorption and reaction on alloy catalyst surfaces I: instrumentation, *Surf. Sci.* 600 (2006) 3028–3035.
- [18] P.A.J. Bagot, A. Cerezo, G.D.W. Smith, 3D atom probe study of gas adsorption and reaction on alloy catalyst surfaces II: results on Pt and Pt-Rh, *Surf. Sci.* 601 (2007) 2245–2255.
- [19] P.A.J. Bagot, A. Cerezo, G.D.W. Smith, 3D atom probe study of gaseous adsorption and reaction on alloy catalyst surfaces III: ternary alloys—NO on Pt-Rh-Ru and Pt-Rh-Ir, *Surf. Sci.* 602 (2008) 1381–1391.
- [20] L. Heezen, V.N. Kilian, R.F. van Slooten, R.M. Wolf, B.E. Nieuwenhuys, NO reduction and adsorption intermediates on Pt-Rh alloy catalysts, *Stud. Surf. Sci. Catal.* 71 (1991) 381–393.
- [21] G.B. Fisher, C.L. DiMaggio, D.D. Beck, Surface chemistry for automotive emissions control: interactions of nitric oxide on a (111) Pt-Rh alloy surface, *Stud. Surf. Sci. Catal.* 75 (1993) 383–396.
- [22] H. Hirano, T. Yamada, K.I. Tanaka, J. Siera, B.E. Nieuwenhuys, The reduction of nitric oxide by hydrogen over Pt, Rh and Pt-Rh single crystal surfaces, *Stud. Surf. Sci. Catal.* 75 (1993) 345–357.
- [23] M. Sheintuch, J. Schmidt, Bifurcations to periodic and aperiodic solutions during ammonia oxidation on a platinum wire, *J. Phys. Chem.* 92 (1988) 3404–3411.
- [24] J. Barcicki, A. Wojnowski, Oscillatory phenomena during ammonia oxidation in the presence of a PtRh catalyst, *React. Kinet. Catal. Lett.* 9 (1978) 59–64.
- [25] C.G. Takoudis, L.D. Schmidt, Dilution effects in the dynamics of ammonia oxidation on platinum with an inert or a product species in the feed mixture, *J. Catal.* 84 (1983) 235–239.
- [26] M.S. Mousa, A. Hammoudeh, J. Loboda-Cackovic, J.H. Block, The CO-oxidation on Pd-rich surfaces of PdCu(110): hysteresis in reaction rates, *J. Mol. Catal. A: Chem.* 96 (1995) 271–276.
- [27] S.Y. Shvartsman, E. Schütz, R. Imbihl, I.G. Kevrekidis, Dynamics of catalytic reactions on microdesigned surfaces, *Catal. Today* 70 (2001) 301–310.
- [28] F. Lovis, T. Smolinsky, A. Locatelli, M.A. Niño, R. Imbihl, Chemical waves and rate oscillations in the H<sub>2</sub> + O<sub>2</sub> reaction on a bimetallic Rh(111)/Ni catalyst, *J. Phys. Chem. C* 116 (2012) 4083–4090.
- [29] T. Smolinsky, M. Homann, R. Imbihl, Tuning excitability by alloying: the Rh(111)/Ni/H<sub>2</sub> + O<sub>2</sub> system, *Phys. Chem. Chem. Phys.* 18 (2016) 970–973.
- [30] V.V. Gorodetskii, B.E. Nieuwenhuys, W.M.H. Sachtler, G.K. Borek, Adsorption of oxygen and its reaction with carbon monoxide and hydrogen on rhodium surfaces. Comparison with platinum and iridium, *Appl. Surf. Sci.* 7 (1981) 355–371.
- [31] B.E. Nieuwenhuys, Adsorption and reactions of CO, NO, H<sub>2</sub> and O<sub>2</sub> on group VIII metal surfaces, *Surf. Sci.* 126 (1983) 307–336.
- [32] P.A. Thiel, T.E. Maday, The interaction of water with solid surfaces: fundamental aspects, *Surf. Sci. Rep.* 7 (1987) 211–385.
- [33] N.M.H. Janssen, A. Schaak, B.E. Nieuwenhuys, R. Imbihl, Unusual behaviour of chemical waves in the NO + H<sub>2</sub> reaction on Rh(111): long-range diffusion and formation of patches with reduced work function, *Surf. Sci.* 364 (1996) L555–L562.
- [34] R.M. van Hardeveld, R.A. van Santen, J.W. Niemantsverdriet, The adsorption of NH<sub>3</sub> on Rh(111), *Surf. Sci.* 369 (1996) 23–35.
- [35] P. Gaspard, The correlation time of mesoscopic chemical clocks, *J. Chem. Phys.* 117 (2002) 8905–8916.
- [36] R. Ishii, K. Matsumura, A. Sakai, T. Sakata, Work function of binary alloys, *Appl. Surf. Sci.* 169–170 (2001) 658–661.
- [37] J. Siera, B.E. Nieuwenhuys, H. Hirano, T. Yamada, K.I. Tanaka, Mechanism of the ammonia formation from NO-H<sub>2</sub>. A model study with Pt-Rh alloy single crystal surfaces, *Catal. Lett.* 3 (1989) 179–190.
- [38] M. Moors, T. Visart de Bocarmé, N. Kruse, Surface reaction kinetics studied with nanoscale lateral resolution, *Catal. Today* 124 (2007) 61–70.
- [39] A.G. Makeev, B.E. Nieuwenhuys, Mathematical modeling of the NO + H<sub>2</sub>/Pt(100) reaction: surface explosion, kinetic oscillations and chaos, *J. Chem. Phys.* 108 (1998) 3740–3749.
- [40] H. Hirano, T. Yamada, K.I. Tanaka, J. Siera, P. Cobden, B.E. Nieuwenhuys, Mechanisms of the various nitric oxide reduction reactions on a platinum-rhodium (100) alloy single crystal surface, *Surf. Sci.* 262 (1992) 97–112.
- [41] K.D. Gibson, J.I. Colonell, S.J. Sibener, The decomposition of NO<sub>2</sub> on Rh(111): product NO velocity and angular intensity distribution, *Surf. Sci.* 443 (1999) 125–132.
- [42] N. Kruse, A. Gaussmann, Adsorbate-induced structural changes of Rh field emitter tips, *Appl. Surf. Sci.* 67 (1993) 160–165.
- [43] E.W. Müller, T.T. Tsong, *Field Ion Microscopy Principles and Applications*, American Elsevier Publishing Company, Inc., New York, 1969.